Indian J Phys (June 2014) 88(6):577–583
DOI 10.1007/s12648-014-0454-1

ORIGINAL PAPER

Highly responsive carbon dioxide sensing by graphene/Al_2O_3 quantum dots composites at low operable temperature

K R Nemade and S A Waghuley*

Department of Physics, Sant Gadge Baba Amravati University, Amravati 444 602, Maharashtra, India

Received: 14 November 2013 / Accepted: 24 January 2014 / Published online: 21 February 2014

Abstract: Novel chemiresistive gas sensors based on graphene/Al_2O_3 quantum dots composites were fabricated and examined for carbon dioxide sensing. Composite samples with different wt% of graphene (20–80 wt%) mixing in constant 1 g Al_2O_3 were prepared and characterized by X-ray diffraction, transmission electron microscopy along with selected area electron diffraction, ultraviolet–visible spectroscopy, fluorescence spectroscopy and thermo gravimetric-differential thermal analysis. The experimental results showed that the graphene/Al_2O_3-based chemiresistor exhibited much higher sensing response and it enhanced linearly with addition of graphene. The gas sensing mechanism was discussed on the basis of defect chemistry through fluorescence measurements. 80 wt% graphene/Al_2O_3 composite exhibited good sensing response (10.84) at room temperature, low operating temperature (398 K), fast response time (14 s) and recovery time (22 s) along with good stability.

Keywords: Graphene/Al_2O_3 composites; Chemiresistor; Sensing response; Operating temperature

PACS Nos.: 07.07.Df; 78.67.Sc; 81.07.Ta

1. Introduction

In recent years, global warming and climate change has been received extensive attention. Ocean absorbing carbon dioxide (CO_2) from the atmosphere results in ocean acidification and subsequently cause to climate change [1]. Likewise, CO_2 is potent greenhouse gas released to the atmosphere by human activities through combustion of fossil fuels to generate electricity, transportation and industrialization. In addition, CO_2 leads to diseases like chronic asthma and bronchitis [2]. Therefore, development of low-cost CO_2 sensors for a continuous and effective monitoring is required [3].

Graphene has attracted much interest due to its outstanding electrical [4] and mechanical properties [5]. Graphene has excellent gas sensing properties due to its high surface to volume ratio [6]. Schedin et al. [7] have developed field-effect transistors to detect the absorption of a single gas molecule. Graphene doped with metal oxides can considerably modify their electronic properties and put forward more surprising results [8].

Metal oxides like SnO_2 [9], ZnO [10], TiO_2 [11] and In_2O_3 [12] are the most efficient CO_2 gas sensing materials. Normally, metal oxide gas sensors are operated at high temperature. This significantly increases power consumption with an increase in operation cost. Al_2O_3 is presently one of the most practical oxide ceramics, as it has been used in many fields of engineering such as heat-resistant materials, coatings, advanced ceramics and cutting materials [13, 14]. Konttinen et al. [15] have reported another interesting characteristic of Al_2O_3, which is moisture resistance. They have shown that Al_2O_3 based sensors are not affected by humidity strappingly. The Al_2O_3 is one of the most important ceramic materials with a range of applications such as chemical sensors [9] and fuel cells [16]. Fan et al. [17] have reported Al_2O_3/graphene nanocomposite and explore its electrical properties. Jiang et al. [18] fabricated and tested Al_2O_3/graphene nanocomposite sensors for ethanol sensing. Venkatesan et al. [19] have reported the stacked graphene-Al_2O_3 nanopore sensors for sensitive detection of DNA and DNA–protein complexes.

Recently, experimental investigations demonstrated that sensing properties are significantly affected by defects

*Corresponding author, E-mail: sandeepwaghuley@sgbau.ac.in

concentration on sensing surface [20, 21]. Thus, the analysis of sensing properties done through defects chemistry by fluorescence measurements and it is extremely suitable approach. Nemade et al. [22] have demonstrated CO_2 sensing by few layered graphene. Yoon et al. [23] have synthesized graphene by stamping method and tested CO_2 sensing properties. Similarly, Nemade et al. [24] have reported graphene/Y_2O_3 quantum dots composite based CO_2 gas sensor. In present investigation, we have found some interesting results over the pristine graphene based sensors.

The present work is planned to investigate CO_2 gas sensing characteristics of graphene/Al_2O_3 quantum dots (QDs) composites. There are few reports related to graphene/Al_2O_3 nanocomposite and it is for the first time, we have explored graphene/Al_2O_3 QDs composites as a CO_2 sensing material. The CO_2 sensing performance of materials is studied at room temperature as well as at different temperatures. The present work is devoted to the detection of low CO_2 concentration. Detection of lower CO_2 concentration is crucial, to monitor environmental pollutant released due to human activities. Some attractive accomplishments are reported; such as chemiresistor have high sensing response, low operating temperature, fast response and good stability.

2. Experimental details

Graphene was obtained by previously reported method [22]. Aluminium oxide (Al_2O_3) QDs was synthesized by chemical route using aluminium nitrate ($Al(NO_3)_2$) and hexamethylenetetramine (HMT) of an analytical grade. The 1 M $Al(NO_3)_2$ was added into 1 M HMT in aqueous medium. The solution was thoroughly mixed by magnetic stirrer for 2 h at room temperature. Subsequently, the product was kept for a centrifuge operating at 3,000 rpm for 30 min. This centrifuged precipitate was collected through cellulose nitrate filter paper. The filtrate was dried at room temperature for over night in vacuum chamber and then sintered at 773 K for 3 h.

The graphene/Al_2O_3 QDs composites were prepared by varying the wt% of graphene in constant 1 g Al_2O_3 QDs using acetone media. The solution was thoroughly mixed by magnetic stirrer for 30 min at room temperature. After this procedure, the solution was kept for over night for evaporation of acetone. In this manner, prepared composite was sintered at 373 K for 1 h for complete evaporation of acetone. It was considered as direct and efficient approach for preparation of graphene/metal oxide composites [25–27]. Four samples were prepared by altering the wt% of graphene from 20 to 80 wt%.

The structural purity of prepared materials was evaluated by X-ray diffraction (XRD) analysis with CuK_α radiation ($\lambda = 1.5406$ nm) (Rigaku Miniflex). The high resolution-transmission electron microscopy (HR-TEM) along with selected area electron diffraction (SAED) was performed to analyse the morphology (Philips Tecnai F-30107). Optical characterizations were done using ultraviolet–visible (UV–VIS) spectrophotometer (Perkin Elmer) and fluorescence Spectrophotometer (Hitachi, F-7000). The thermo gravimetric-differential thermal analysis (TG–DTA) was obtained in a Shimadzu DTG-60 h thermal analyser. The TG–DTA measurement was carried out from room temperature to 775 K in nitrogen atmosphere.

The synthesized samples were used as sensing layer. The chemiresistors of as-prepared samples were fabricated by screen-printing technique on glass substrate of size 25 mm × 25 mm and drying under controlled temperature rate up to 343 K. The silver electrodes were deposited on adjacent sides of the film for the measurement of the electrical resistance. CO_2 sensing properties of materials were studied in a homemade gas sensor assembly. Humidity and temperature within the chamber were precisely controlled. The sensing response was studied by using air as background gas having H_2O lower than 2 ppm. The known volume of the CO_2 was inserted into the gas chamber to maintain required concentration inside the chamber. Each reading of chemiresistor have acquired after period of 10 s. Resistance of the chemiresistor was measured by using a voltage divider method [28]. The sensing response of chemiresistor was defined as [27]:

$$S = \frac{\Delta R}{R_a} = \frac{|R_g - R_a|}{R_a} \quad (1)$$

where R_a and R_g is the resistance of chemiresistor in air and gas, respectively.

3. Results and discussion

X-ray diffraction (XRD) patterns of graphene, Al_2O_3 QDs and (20–80 wt%) graphene/Al_2O_3 QDs composites are shown in Fig. 1. Diffraction peaks in the patterns Fig. 1(a), and 1(b) are in agreement with standard XRD peaks, which confirm the formation of graphene (JCPDS No. 01-0646) and Al_2O_3 (JCPDS 10-0173), respectively. We have not observed presence of any peaks due to impurities. Reflecting planes observed in graphene and Al_2O_3 QDs appear at the same positions in composites, curves shown in Fig. 1(c)–1(f), indicating good coordination between the components of the composites; i.e. graphene and Al_2O_3 QDs. The crystallite size obtained using Debye–Scherrer formula. Average crystallite size of Al_2O_3 QDs is found to be 5.5 nm and for composites, it is in the range 3.23–4.41 nm. The smallest crystallite size is found to be 3.23 nm for 80 wt% graphene/Al_2O_3 QDs composite.

Figure 2(a) depicts TEM image of the synthesized Al_2O_3 QDs. The small amount of agglomeration is present in the sample. Average crystallite size estimated from the TEM analysis agrees with that obtained from XRD analysis. Diffraction spots shown in SAED image presented in Fig. 2(b), agreeing with the results obtained from XRD analysis. The several diffracting rings (012), (104), (110), (113) are identified in the diffraction patterns.

Figure 3(a) and 3(b) shows TEM and SAED images of 80 wt% graphene/Al_2O_3 composites, respectively. Broad rings in Fig. 3 are indicative of the good coordination between graphene and Al_2O_3 QDs. From magnified image shown in Fig. 3(c), it is observed that Al_2O_3 QDs are attached to surface and edges of graphene. Hybridised structure of Al_2O_3 QDs and graphene has been directly visualised in HR-TEM, shown in Fig. 3(d). Well-defined lattice fringes of the Al_2O_3 QDs are clearly observable.

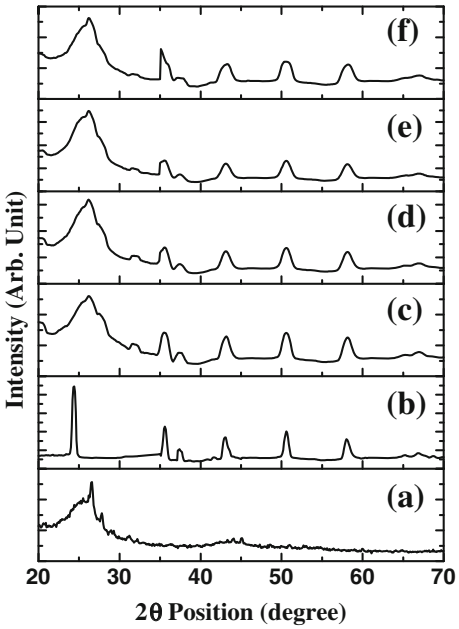

Fig. 1 XRD patterns for (*a*) graphene, (*b*) Al_2O_3 QDs along with (*c*) 20 wt%, (*d*) 40 wt%, (*e*) 60 wt% and (*f*) 80 wt% of graphene/Al_2O_3 QDs composite

UV–VIS spectra of graphene and Al_2O_3 QDs are shown in Fig. 4. The spectrum of graphene shows intense absorption at 268 nm, which is attributed to the C–C bonds in graphene [29]. UV–VIS spectroscopy gives definite idea about the quantum confinment, which is an intrinsic characteristics of quantum dots [30]. UV–VIS spectrum of Al_2O_3 QDs shows an intense absorption at 355 nm. The average crystallite size of Al_2O_3 estimated from XRD and TEM analysis is 5.5 nm and absorption in UV region confirms that the synthesized particles are quantum dots [31].

The emission spectra of 20–80 wt% graphene/Al_2O_3 composites, have been recorded under 254 nm irradiation in the range 315–700 nm, are shown in Fig. 5. Defect density has been directly estimated using the intensities ratio of the ultraviolet (I_{UV}) to visible deep levels (I_{DL}) [20]. I_{UV}, I_{DL} and I_{UV}/I_{DL} values are listed in Table 1. Oxygen vacancies are the most probable point defects, which increase the probability of adsorption of oxygen on sensing surface [21].

Figure 6 shows TG–DTA profile of 80 wt% graphen/Al_2O_3 QDs composites. The significant mass loss is observed below 373 K and DTA curve shows an endothermic peak at 346 K due to the evaporation of absorbed water. The total mass loss from room temperature to 473 K is about 10.20 %. The DTA curve show another peak at 541 K which corresponds to the evaporation of the constitution water in Al_2O_3 QDs. The exothermic peak appears at 705 K, which may be associated with the phase change of α-Al_2O_3 → θ-Al_2O_3 in composite [32]. TG–DTA study shows that the material is stable in temperature range from 350 to 500 K. Beyond 500 K, the mass starts to decrease smoothly, suggesting the pyrolysis of the carbon component of the composite.

Figure 7 shows the comparative gas sensing response of chemiresistors measured with CO_2 and liquid petroleum

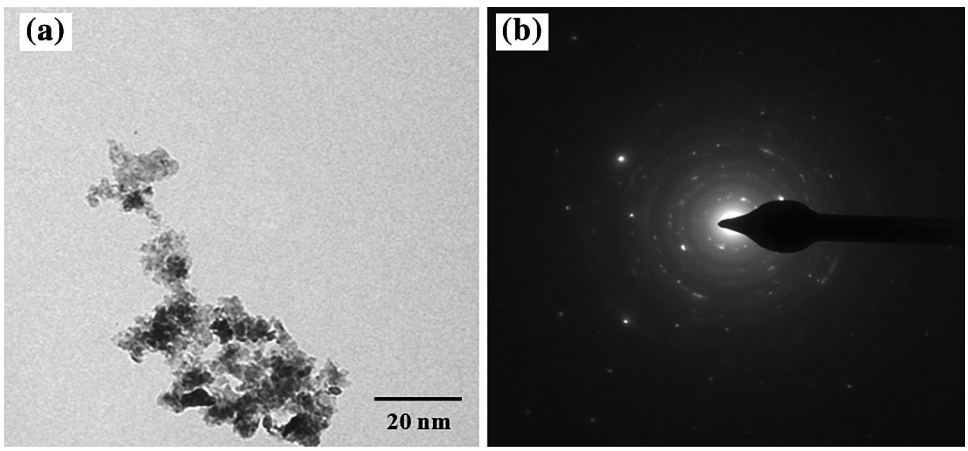

Fig. 2 (**a**) TEM and (**b**) SAED image for Al_2O_3 QDs

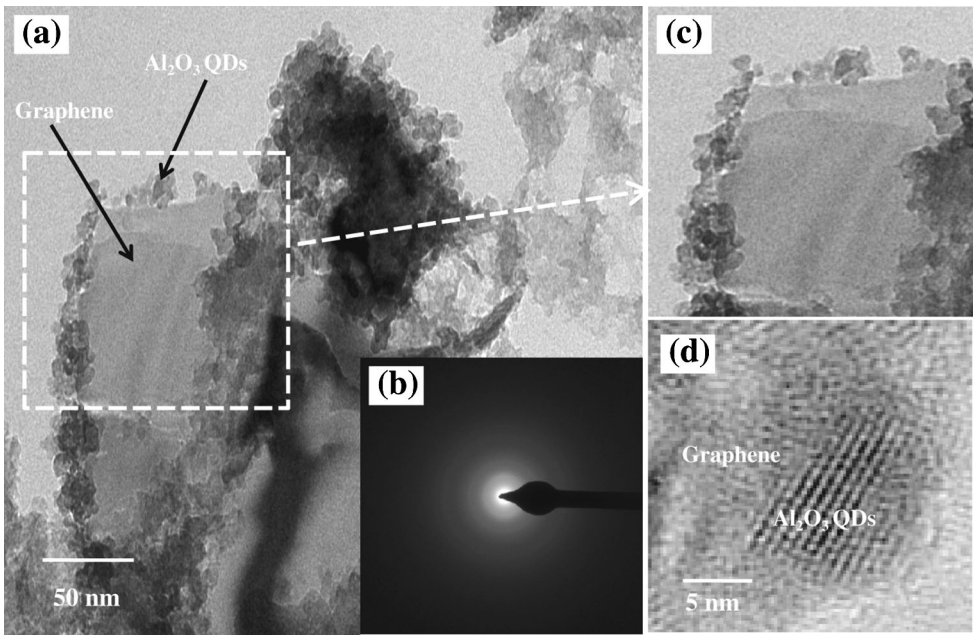

Fig. 3 (**a**) TEM (**b**) SAED image (**c**) Magnified image of the *red section* in *panel* **a**. (**d**) HR-TEM image for hybridised structure of 80 wt% graphene/Al_2O_3 QDs composite

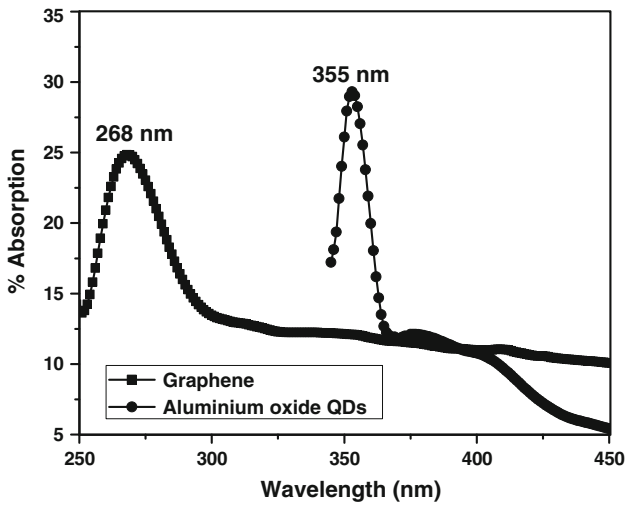

Fig. 4 UV-VIS spectra for graphene and Al_2O_3 QDs

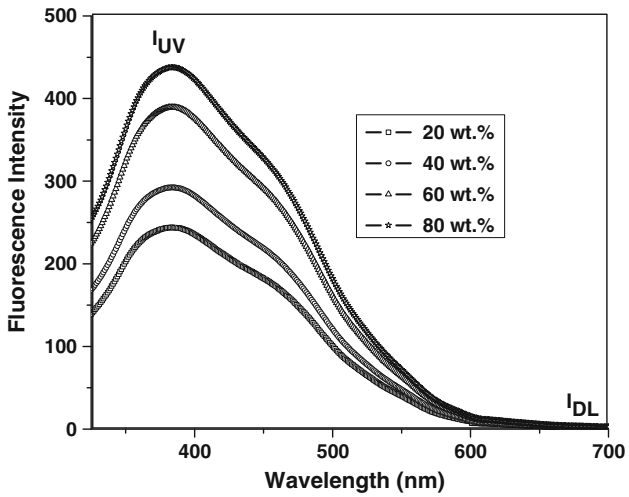

Fig. 5 Fluorescence spectra for 20–80 wt% graphene/Al_2O_3 QDs composites

gas (LPG) for 40 ppm at 398 K. All chemiresistors possess more than 50 % response for CO_2 and this value is 96 % for 80 wt% chemiresistor. This result shows that chemiresistors are more selective towards CO_2 as compared to LPG.

The gas sensing response of chemiresistors as a function of CO_2 concentrations at room temperature (298 K) is shown in Fig. 8. Chemiresistors exhibit an increase in response as a function of CO_2 concentration up to 200 ppm. This indicates that chemiresistors demonstrate a good dependence on the gas concentrations. As discussed in introduction section, humidity does not hinder the performance of Al_2O_3 based gas sensors. Moreover, the response of (20–80 wt%) graphene/Al_2O_3 QDs composites chemiresistors is almost linear. From Fig. 8, it is clearly evident that composition with 80 wt% graphene/Al_2O_3 has the maximum sensing response. To evaluate reproducibility of the results, each measurement has been repeated 5 times and insignificant deviation is observed in the results. This may be due the smaller crystallite size, which provides a larger surface area for gas–solid interaction [33]. Figure 8 also clearly shows an enhancement in sensing response obtained with the increase in wt% of graphene. The XRD studies reveal that there is no significant difference between the particle sizes of composites. Therefore, it is necessary to concentrate on defect density that affects sensing response. The defect density on the sensing surface is determined by I_{UV}/I_{DL} ratio using fluorescence

Table 1 (I_{UV}/I_{DL}) ratio for 20–80 wt% graphene/Al_2O_3 QDs composites

Wt% of graphene	I_{UV}	I_{DL}	I_{UV}/I_{DL}
20	243	3.51	69.23
40	292	3.6	81.11
60	387	3.57	108.40
80	437	3.62	120.71

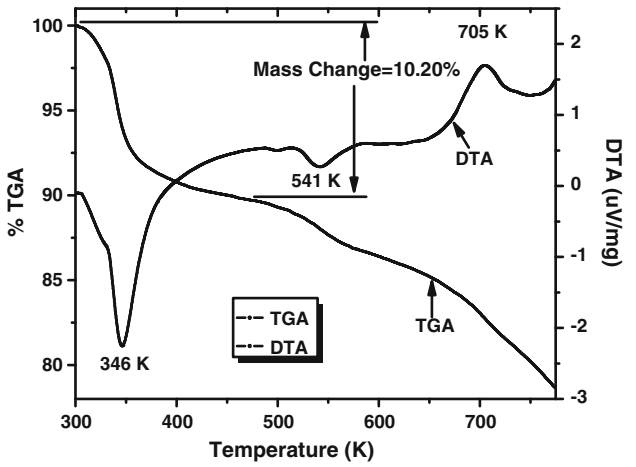

Fig. 6 TG and DTA curves for 80 wt% of graphene/Al_2O_3 QDs composite

mesurments. From Table 1, it is directly observed that density of defects (I_{UV}/I_{DL}) increases with an increase in wt% of graphene. Figure 9 shows variation of (I_{UV}/I_{DL}) ratio and CO_2 sensing response as a function of wt% of graphene.

It is observed that excellent correlation exists between I_{UV}/I_{DL} ratio and gas sensing response. It also shows that defects density linearly increase with wt% of graphene. Density of defects may increase due to damage to graphene surface during addtion of graphene into Al_2O_3, or by interaction between Al_2O_3 and graphene which may create vacancies or dangling bonds. Incraesing the amount of graphene added into fixed amount of Al_2O_3, i.e. increasing number of graphene sheets becomes defective. Thus, defective sites of the graphene increase, where an adsorption energy increases. Hence, gas sensing response is influenced by defects concentration and is linelarly proportinal to the defect density. This result is consistent well with the results reported early by [21, 34]. The gas sensing response is related to defects through the oxygen vacancies, which can act as adsorption sites for atmospheric oxygen during gas sensing. More is the number of defects, more oxygen ions are adsorbed. This is one of the possible reasons for increase in sensing response with an increase in defects density.

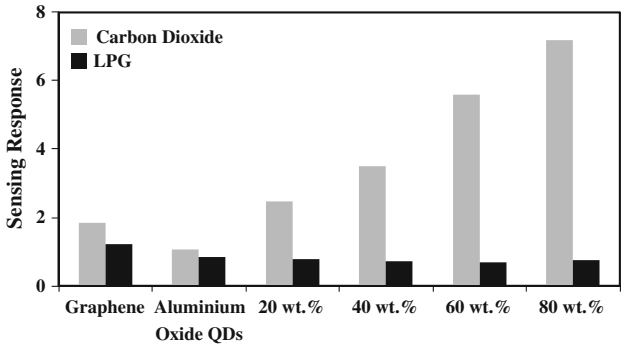

Fig. 7 Comparative gas sensing responses of chemiresistors towards CO_2 and LPG for 40 ppm at 398 K

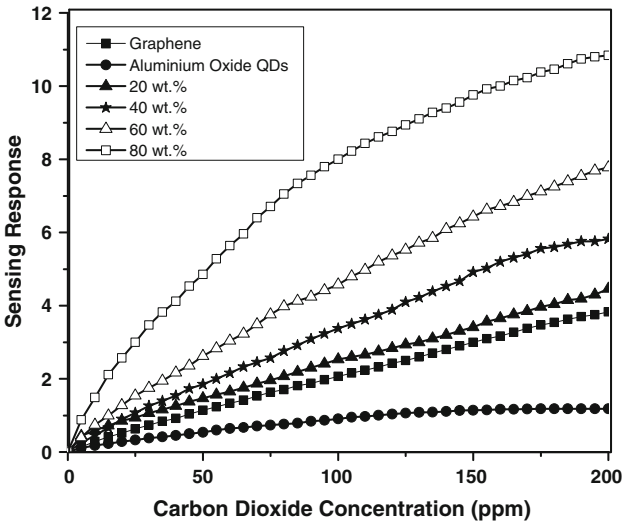

Fig. 8 Variation of response of chemiresistors with the concentration of CO_2 at room temperature

Oxygen adsorbed on the surface of sensing material is mainly involved in sensing process of CO_2. The reaction for adsorbed oxygen ions are as follows [35].

$$O_2(\text{gas}) \rightarrow O_2(\text{ads}) \quad (2)$$

$$O_2(\text{ads}) + e^- \rightarrow O_2^-(\text{ads}) \quad (3)$$

$$O_2^-(\text{ads}) + e^- \rightarrow 2O^- \ (\text{ads}) \quad (4)$$

CO_2 gas sensing mechanism is based on the reaction between the surface of chemiresistors and adsorbed oxygen ions. CO_2 has strong electron injecting tendency. Upon exposure to CO_2 (oxidising gas) environment, CO_2 molecules is adsorbed on bridging oxygen atoms with the formation of a surface carbonates and increase the resistance of chemiresistor indicating that sensing materials have *n*-type characteristics [36, 37].

The response of chemiresistors (graphene, Al_2O_3 QDs and 20–80 wt% graphene/Al_2O_3 QDs composites) as a function of operating temperature towards 50 ppm CO_2 is

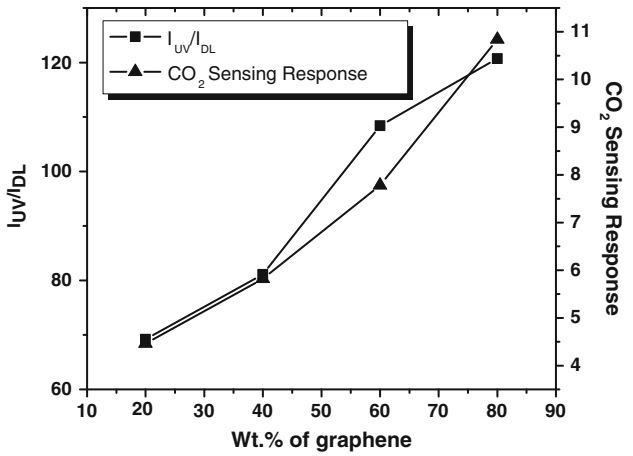

Fig. 9 Variation of I_{UV}/I_{DL} ratio and CO_2 sensing response with wt% of graphene

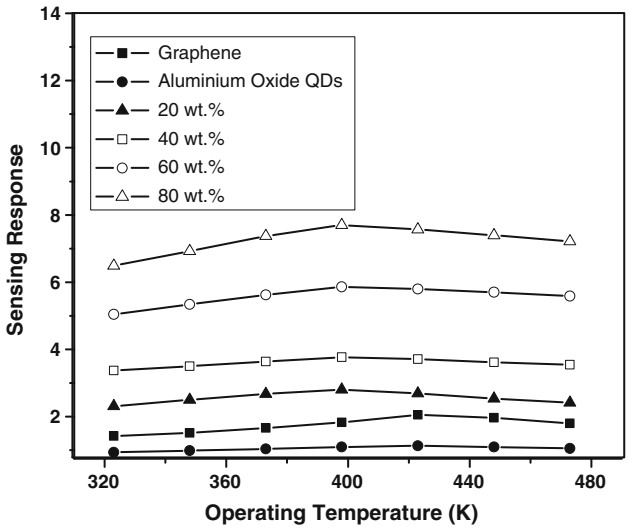

Fig. 10 Sensing response of graphene, Al_2O_3 QDs and 20–80 wt% graphene/Al_2O_3 chemiresistors as a function of operating temperature

shown in Fig. 10. Response of chemiresistors to CO_2 varies with amount of wt% graphene and temperature. It is observed that 80 wt% graphene/Al_2O_3 composites exhibit the maximum value of sensing response at 398 K. This shows that the effect of graphene is significant. From Fig. 10, it is observed that all composites possess same operating temperature at relatively low temperature than pure graphene and Al_2O_3. Lower operating temperature would result in low power consumption. This is the main accomplishment of present work. Here, operating temperature 398 K fits in thermal stability domain of sensing material, which is comprehensively supported by TG–DTA. However, sensing response smoothly declines above 398 K. This may be due to desorption of oxygen ions from chemiresistor surface. When thermal vibration becomes

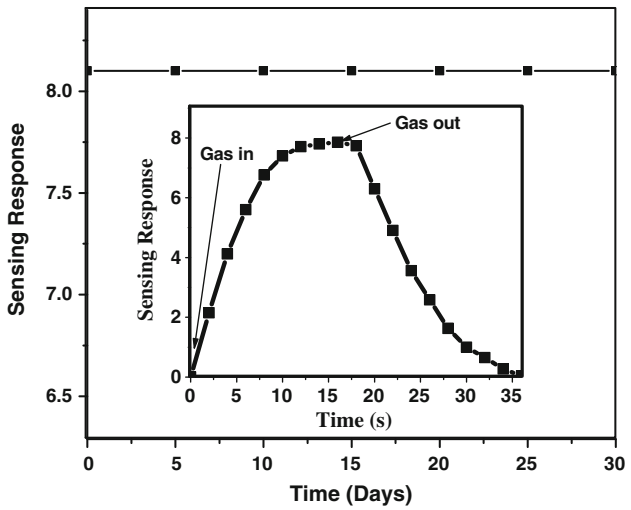

Fig. 11 Stability characteristics of 80 wt% graphene/Al_2O_3 chemiresistor to 100 ppm CO_2. Inset shows Transient response of 80 wt% graphene/Al_2O_3 chemiresistor to 100 ppm CO_2

sufficient, adsorbed oxygen gets desorbed [34]. Also at high temperatures, chemiresistors experience a continuous drift in resistance value [38].

In order to check the stability of 80 wt% graphene/Al_2O_3 chemiresistor, its response to 100 ppm CO_2 has been measured for 30 days, at an interval of 5 days. Stability response result is shown in Fig. 11. Chemiresistor has almost constant sensing response indicating the excellent stability. Combining results obtained for all above-mentioned sensing properties, 80 wt% graphene/Al_2O_3 QDs composite is a potential sensing material to be used for efficient sensing of CO_2.

Transient response of the 80 wt% graphene/Al_2O_3 chemiresistor at room temperature to 100 ppm concentration of CO_2 is displayed in the inset of Fig. 11. The time required for resistance to rise from its initial value to 90 % of highest value is known as response time of chemiresistor. The time required for decrease in resistance value to 90 % of highest value known is as recovery time. It is found that the fast response time for chemiresistor to 100 ppm CO_2 is 14 s, and recovery time is 22 s. The difference in response and recovery time may be due to faster CO_2 diffusion [38], while slow recovery due to formation of surface carbonates.

4. Conclusions

In summery, chemiresistors fabricated by using graphene/Al_2O_3 composite through screen-printing method are successfully demonstrated sensitive towards CO_2. Structural and morphological studies the composites indicate good coordination between graphene and Al_2O_3, which results in

an increase in sensing response with the wt% of graphene. Also, the sensing response of chemiresistors shows good dependence on defects density on sensing surface. 80 wt% graphene/Al_2O_3 QDs composite chemiresistor can be used to practical sensor at room temperature and relatively low temperature (398 K).

Acknowledgments Authors are very much thankful to Head, Department of Physics Sant Gadge Baba Amravati University, Amravati for providing necessary facilities. Nemade is thankful to Sant Gadge Baba Amravati University, Amravati for financial support through the Late M N Kale scholarship (2012).

References

[1] C Booth, D McDonald and P Walsh *Marine Biol. Lett.* **5** 347 (1984)
[2] R Desai, D Lakshminarayana, P Patel and C J Panchal *Sens. Actuators B* **107** 523 (2005)
[3] J Herran, G G Mandayo and E Castano *Sens. Actuators B* **129** 705 (2008)
[4] C Bai, J Wang, G Yang and Y Yang *Indian J. Phys.* **87** 133 (2013); Z Wu et al. *Sens. Actuators B* **178** 485 (2013)
[5] A K Geim *Science* **324** 1530 (2009)
[6] H E Romero et al. *Nanotechnology* **20** 245501 (2009)
[7] F Schedin et al. *Nat. Mater.* 6 **652** (2007)
[8] Y Li et al. *J. Am. Chem. Soc.* **134** 15 (2012)
[9] M. Mahdizadeh-Rokhi *Indian J. Phys.* **87** 517 (2013); S A Waghuley *Indian J. Pure Appl. Phys.* **49** 816 (2011)
[10] G Y Chai et al. *Sens. Actuators A* **176** 64 (2012)
[11] G Telipan, M Ignat, C Tablet and V Parvulescu *Adv. Mater.* **10** 2138 (2008)
[12] G Jimenez-Cadena, J Riu and F X Rius *Analyst* **132** 1083 (2007)
[13] P K Panda, V A Jaleel and G Lefebvre *Mater. Sci. Engineering A* **485** 558 (2008)
[14] N P Damayanti *J Sol-Gel Sci. Technol.* **56** 47 (2010)
[15] P Konttinen and P D Lund *Sol. Ener. Mater. Solar Cell* **82** 361 (2004)
[16] A S Chellappa, C M Fischer and W J Thomson *Appl. Catal. A* **227** 231 (2002)
[17] Y Fan et al. *Carbon* **48** 1743 (2010)
[18] Z Jiang, J Wang, L Meng, Y Huang and L Liu *Chem. Commun.* **47** 6350 (2011)
[19] B M Venkatesan et al. *ACS Nano* **24** 441 (2012)
[20] O Lupan et al. *Sens. Actuators B* **144** 56 (2010)
[21] S Pati, S B Majumder and P Banerji *J. Alloys Comp.* **541** 376 (2012)
[22] K R Nemade and S A Waghuley *J. Electron. Mater.* **42** 2857 (2013)
[23] H J Yoon, D H Jun, J H Yang, Z Zhou, S S Yang and M M Cheng *Sens. Actuators B* **157** 310 (2011)
[24] K R Nemade and S A Waghuley *Int. J. Modern Phys.: Conf. Series* **22** 380 (2013)
[25] J Liu, H Bai, Y Wang, Z Liu, X Zhang and D D Sun *Adv. Funct. Mater.* **20** 4175 (2010)
[26] M Feng, H B Zhan and Y Chen *Nanotech.* **21** 075601 (2010)
[27] S A Waghuley, S M Yenorkar, S S Yawale and S P Yawale *Sens. Actuators B* **128** 366 (2008)
[28] T Kuila, S Bose, A K Mishra, P Khanra, N H Kim and J H Lee *Prog. Mat. Sci.* **57** 1061 (2012)
[29] K R Nemade and S A Waghuley *Results in Phys.* **3** 52 (2013)
[30] S S Nath, M Choudhury, G Gope and R K Nath *Nanotrends* **8** 1 (2010)
[31] H Ke-long, Y Liang-guo, L Su-qin and L Chao-jian *Trans. Nonferrous Met. Soc.* **17** 633 (2007)
[32] L K Bangal, J Y Patil, I S Mulla and S S Suryavanshi *Ceramics Int.* **38** 4835 (2012)
[33] M W Ahn et al. *Appl. Phys. Lett.* **93** 263103 (2008)
[34] K R Nemade and S A Waghuley *Solid State Sciences* **22** 27 (2013)
[35] J Wang, Y Kwak, I Lee, S Maeng and G Kim *Carbon* **50** 4060 (2012)
[36] K Fan, H Qin, L Wang, L Ju and J Hu *Sens. Actuators B* **177** 265 (2013)
[37] K R Nemade and S A Waghuley *J. Chinese Adv. Mater. Soc.* **1** 219 (2013)
[38] M Morio, T Hyodo, Y Shimizu and M Egashira *Sens. Actuators B* **139** 563 (2009)